Estimation of Specific Absorption Rate (SAR) and Penetration Depth in Cubical Models of Human Head Exposed to Plane Waves in Frequency Range 500-2450 MHz

M. Bahar^{*}; Department of Basic Sciences, Garmsar Branch, Islamic Azad University
H. Golnabi; Institute of Water and Energy, Sharif University of Technology
M. Hamidi; Physics Department, North Tehran Branch, Islamic Azad University

Abstract

The aim of this study was to estimate Specific Absorption Rate (SAR) induced in human head tissues, by assuming human head as a cubical model filled with lossy dielectric material and exposed to electromagnetic plane waves. The research is carried out by computational simulation using C programming codes. The numerical technique used in this study was Finite Difference in Time Domain (FDTD) method, along with Perfectly Matched Layer (PML) as an appropriate absorbing boundary condition. Different conditions including exposure conditions as well as physical parameters are employed, in order to compare the results to the past literature. Finally, the penetration depth of one of the specified models is expressed by means of interpolation. The results which are in complete agreement with the others in some cases, suggests that considering the biological tissues as dispersive media, would result in correct estimations; whereas changing in the structure of the model, doesn't differ if precise predictions are not important. Furthermore, the penetration depth correlation to frequency is in line with what is expressed in theoretical papers.

 Keywords: SAR, mobile phone radiation, FDTD Method, RF Frequencies, Biological tissues

 Received: 29 Oct 2013
 Revised 12 Jan. 2014

 * Correspondence Author
 bahar@khu.ac.ir

Introduction

Nowadays by the development of technology, using electrical devices inevitably results in excessive electromagnetic exposure of human being. It includes domestic sources such as personal wireless devices (mobile phones or pagers) as well as RF dielectric heaters, RF sealers, radars and RF transmitters as industrial or occupational sources. In investigating the effects of the radiation emitted by these sources, there is a classification based on the photons energy during the interaction with matter. Ionizing radiation which has been studied for about sixty years refers mostly to the gamma and X radiation; while the non- ionizing radiation is referred to the lower frequencies of Electromagnetic spectrum and covers the ultra violet waves and lower frequencies. This type of radiation, despite its name has raised more debates in the last 20 years, as some evidences show that the energy of photons in this frequency range are sufficient for some molecular interactions. The non ionizing radiation could be subdivided into other groups such as low frequency fields (LF), Medium frequency fields (MF) and high frequency fields (HF) regarding the area of research. What is more important is that they have biological effects as well as thermal effects, and the theory of the biological effects is still unknown is some cases. [1, 2]

To have a review on the past literature, modeling of the human body and using numerical methods are the main points to be mentioned. The first anatomically realistic voxel model of humans due to the ICRP standards [3] called NORMAN, was developed by P. Dimbylow in 1996 [4]. Later more models, regarding gender, age and different species were introduced by others [5, 6]. What makes us more indebted in this field of study is the database of tissues' dielectric properties, established by Gabriel et al (1996) [7]. This database provides us the conductivity and permittivity of some animals and human tissues in a wide frequency range in addition to some predictions on a model for dielectric spectrum of the tissues, and this would help us on the simulation of human body tissues_ if we consider there is not much difference between human and animal tissues according to the measurements in [8].

The next step for simulating is an efficient numerical method, which can accurately estimate the solution to Maxwell's equations. There have been several numerical methods based on integral or differential equation techniques, and the specification of the domain which could be time or frequency. What is more important in this step is the boundary condition, which could work out the problem more accurate. An appropriate numerical method along with an efficient boundary condition, make the simulation of electromagnetic waves interaction inside the body more satisfactorily. The importance of simulating of electromagnetic waves has made scientists produce some commercial software packages, which are available in some universities or institutions. The numerical method which is applied in most of these packages is the Finite difference in Time Domain (FDTD) method [9]. The boundary conditions used, are also different according to the field of Bioelectromagnetics, as it could be applied for nonhomogeneous, non-isotropic, nonlinear and dispersive media due to an exposure of plane waves [10].

In this study, some major head tissues are exposed to electromagnetic waves within the frequency range of 500- 2450 MHz, and the thermal effects are investigated according to computational calculations. In some stages, few frequencies are selected, since the human head is more exposed to them by proximity of mobile phones. The frequencies are approximately 900 and 1800 MHz and refer to the Global System for mobile communications (GSM) frequency ranges _ popular in most parts of the world.

The wave is simulated as a planar wave field equation, and to comply with some simulation software, in which the dispersive biological tissues are taken into account; we defined a 14.6 cm cubical model with isotropic, homogeneous and lossy dielectric parameters for the human head. The numerical method used is FDTD as well as the PML representing the boundary condition. Various results are obtained due to the variation of initial conditions, such as input power, frequency and model layers. The correlation of penetration depth to frequency is finally estimated, by considering grey matter as a lossy dielectric medium. It should be noted that, the simulation is undertaken in C# codes, while the final data are plotted in MATLAB view for more data analysis.

Materials and Methods

1. Simulation Process

In the frequency range of 100 kHz to 6 GHz, the dosimetric quantity which is used as an index of comparison and estimation of energy absorption inside the biological tissues, is called Specific Absorption Rate (SAR), and defined as follows

$$SAR = \frac{d}{dt} \left(\frac{dW}{dm} \right) = \frac{d}{dt} \left(\frac{dW}{\rho dV} \right) \quad W/kg$$
 (1)

where, dW is the increment of absorbed or dissipated energy in the mass element of tissue with mass density of ρ (kg/m³). The relation between SAR and the amplitude of electric field is

$$SAR = \frac{\sigma |E^2|}{\rho} \qquad W/kg$$
 (2)

In this equation σ (S/m) is electrical conductivity of tissue, and E is the rms electric field strength (V/m) [11]. The SAR is related to the temperature rise in tissue by

$$SAR = \frac{c\Delta T}{\Delta t}$$
 W/kg (3)

where c is the specific heat of tissue ($J/kg \cdot C^{\circ}$), and Δt is the time interval (seconds) in which temperature increment ΔT is measured.

IEEE and ICNIRP have established some basic restrictions on the rate of energy deposition inside the human head and trunk within the related frequency range, to prevent the thermal effects of such radiation on human, either in occupational or public scale. The guidelines determine that the average SAR in any 10 gr region of body tissues shouldn't exceed 10 W/kg at occupational or 2 W/kg at public exposures [12]. According to these standards, ΔT should not exceed 1 C°.

To estimate SAR in a biological tissue, what we need first is the solution to the Maxwell's electromagnetic equations inside the physical medium. Those could be either the differential equations or the integral ones. Among the numerous techniques which provide a numerical solution to these equations, the Finite Difference in Time Domain (FDTD) method, which was first introduced by K.S. Yee (1966), seems to be the best method for our study, since it could be applied to find the solutions quickly as well as being coded into computer programs quite easily. Furthermore it has been mentioned in some reference books that the FDTD method is more applicable in bioelectromagnetic

researches, since it is extremely versatile in whole body or partial body exposures, due to various spatial fields (far or near fields) as well as other initial conditions [13], [14].

Maxwell's differential equations for an isotropic medium, which has no electric or magnetic sources but may have materials that cause electric or magnetic losses are as follows

$$\frac{\partial \mathbf{D}}{\partial t} = \nabla \times \mathbf{H} - \mathbf{J}_{\mathbf{e}}$$
(4)

$$\frac{\partial \mathbf{B}}{\partial t} = -\nabla \times \mathbf{E} - \mathbf{J}_{\mathbf{m}}$$
(5)

in which $\mathbf{D} = \varepsilon \mathbf{E} = \varepsilon_r \varepsilon_o \mathbf{E}$, $\mathbf{B} = \mu \mathbf{H}$, $\mathbf{J_e} = \sigma \mathbf{E}$ and $\mathbf{J_m} = \sigma^* \mathbf{H}$. Besides ε and μ are also permittivity and permeability of the medium as well as σ and σ^* which are the electric conductivity and the equivalent magnetic resistivity of the medium respectively. Working in Cartesian coordinates system, we can derive 6 scalar equations from the equations (4) and (5), including partial space and time derivatives for E and H intensities. These terms could be then expressed by employing the spatial and temporal derivatives equivalences, represented by Yee in the FDTD method [11].

In this method, the whole volume of interest is subdivided into a grid of Yee cells. The grid coordinates are incremented by Δx , Δy and Δz as well as the time, which is incremented by Δt , while n represents time steps and is an integer. Taking Yee's approach, we can then determine **E** (or **H**) at any position inside the medium from their previous values at the adjacent grid positions. By the time intervals, we can also find out how much the energy is absorbed inside the body as the time passes.

In order to achieve the necessary accuracy, the minimum spatial increments of the Yee's cells are determined to be 10- 20 samples per wavelength. What we have proposed for a cubical cell in this study is the minimum value due to the maximum number of samples,

$$\Delta x = \Delta y = \Delta z \le \frac{c_0}{20 f \sqrt{\epsilon_r}} \tag{6}$$

in which f is the applied wave frequency, ε_r is the relative permittivity of the tissue, and c_0 is the light velocity in free space. Moreover, temporal sampling should be sufficiently small, in order to maintain the stability of the FDTD method, which is named the Stability Criterion by Yee [9],

$$\Delta t \le \frac{1}{c_0 \sqrt{\frac{1}{\Delta x^2} + \frac{1}{\Delta y^2} + \frac{1}{\Delta z^2}}}$$
(7)

Considering equal size for cubical cells, we can then write down the following equation instead of equation (7),

$$\Delta t \le \frac{\Delta x}{c_0 \sqrt{3}} \tag{8}$$

The next step to carry out the simulation is to terminate the mesh in a way that the computational domain is reduced, while no reflection from the medium boundaries interferes the calculations. Various types of absorbing boundary conditions have been presented on this issue using analytical techniques. Among all, the Perfectly Matched Layer (PML) is a highly effective method introduced by Berenger in (1994). This approach, which is known as an artificial boundary condition, could be imposed in different media, as well as being exposed by different plane waves. Using the instructions can lead to solutions to the Maxwell's equations inside this layer [10]. Subsequently, by applying the Yee algorithm for this layer, the program would be accomplished in sampling basis.

The final step to estimate energy absorption rate inside the medium is to define physical and dielectric properties of the tissues proposed to study. It is known that biological tissues are types of dispersive media, following the dielectric spectrum described by Gabriel et al [7] in terms of multiple Cole- Cole equations and a conductivity term as shown below,

$$\widehat{\varepsilon_{r}}(\omega) = \varepsilon_{\infty} + \sum_{n=1}^{4} \frac{\Delta \varepsilon_{n}}{1 + (i\omega\tau_{n})^{1-\alpha}} + \frac{\sigma_{s}}{i\omega\varepsilon_{\circ}}$$
(9)

in this equation, ε_{∞} is the permittivity at field frequencies where $\omega \tau \gg 1$, and ε_{\circ} is the permittivity of free space. $\Delta \varepsilon_{n} = (\varepsilon_{s} - \varepsilon_{\infty})$ is expressed as the magnitude of dispersion, while ε_{s} is the permittivity at frequencies where $\omega \tau \ll 1$. In addition to that, **n** refers to each dispersion regions of the tissue's main constituents, as well as τ_{n} which refers to the relevant relaxation times. This model is known to be a complex equation, regarding $i^{2} = -1$ and *a* as a real constant in the range [0, 1]. It should be

added that the magnetic properties of biological materials are different from one to another; however most of them are regarded as diamagnetic.

Taking all the above into the program, by some other specifications such as incident wave characteristics, the source location, and other physical specifications of the tissue, we can then find SAR at any position inside the medium, and that would consequently help us on further research on the issue.

2. Specifications of the model used in this study

Assuming the human head as a cube of 14.6 cm in size, which is the average size of an adult [3, 15], filled with an isotropic and homogeneous lossy dielectric material; we can express the dielectric spectrum of the model as,

$$\widehat{\varepsilon_{\rm r}}(\omega) = \varepsilon_{\infty} + \frac{\sigma_{\rm s}}{\mathrm{i}\omega\varepsilon_{\circ}} \tag{10}$$

which is the combination of the first and third terms of equation (10). Subsequently, the necessary parameters would be taken into account during the research according to table (1). Furthermore, the permeabilities of the tissues are considered to be equal to that of free space.

This model is used during 3 stages of the research; while in one another stage the model is changed into a multi planar layered cube of the same size, including different isotropic and homogeneous lossy dielectric materials [figures [1- (a, b)].

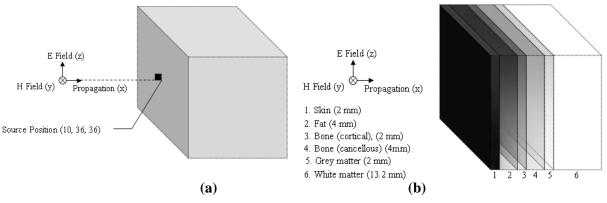


Figure1. a) Simple model exposed to plane waves at source position,b) Multi layered planar model used in this study

According to equation (6), the cells sizes imposed in the models follow below,

$$\Delta x = \Delta y = \Delta z = \frac{3 \times 10^8 \,(\text{m/s})}{20 \times 2450 \times 10^6 \,(1/\text{s}) \times \sqrt{4}} = 3.1 \,\text{mm}$$
(11)

which is the minimum size acquired during this study. Consequently, the maximum time increment due to equation (8) is,

$$\Delta t = \frac{3.1 \times 10^{-3} \text{ (m)}}{3 \times 10^8 \text{ (m/s)} \times \sqrt{3}} = 5.9 \text{ ps}$$
(2)

Having a more detailed SAR distribution, in order to compare the results with past literature on realistic head models, is the reason for setting the above values 2 mm and 3.9 ps respectively.

The incident wave is also proposed to be a planar electromagnetic wave, in different frequencies and powers. The wave enters perpendicularly to the medium at cell number (10, 36, 36) on the left side of the model, and propagates on x- direction as shown in figure (1-a). Furthermore, the electric field (\mathbf{E}) is imposed on z- direction; whereas the magnetic field (\mathbf{H}) is on the y- direction by the values varying due to the input power.

For more details on the wave parameters, it should be mentioned that the radio frequencies used in this study are those of the most incidence toward human head and are propagated by cellular phones antennas. The related carrier frequencies applied by the Global System for Mobile communication (GSM) throughout the world, are approximately 900 and 1800 MHz, and the input powers are 1 and 2 W. It should be noted that, the changes in the battery current of these devices generate extremely low frequency (ELF) magnetic fields in the range of few Hz to 40 kHz, but they are supposed to be within the safety levels [13, 14].

Considering the cell sizes, allocating 7 cells to the PML as well as 2 cells to the air layer on each side, the whole computational domain then consists of $91 \times 91 \times 91$ cells, being sampled every 3.9 (ps) during a period of time, to find the SAR pattern inside the model.

Results

Describing head models, exposure conditions and computational methods, we can now survey energy deposition inside the models from different aspects. There are 5 stages which are carried out in this study.

1. SAR variation in homogeneous models due to different input powers

6 major head tissues are taken into account in this stage to investigate the impact of power changes. The input power is set to be 2 W and 1 W, while the frequency is fixed on 900 MHz. Each tissue is exposed to either of the input powers separately, and the results are then compared.

2. SAR variation in homogeneous models due to different input frequencies

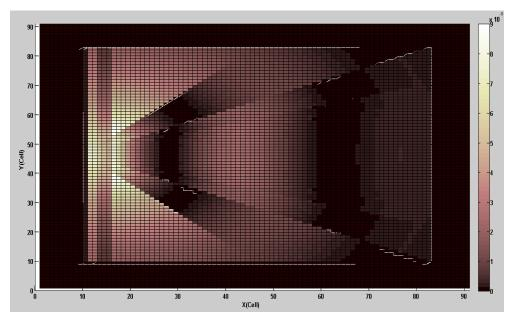
The same procedure is done in this stage, by setting frequencies 900 and 1800 MHz, while the input power is fixed on 2 W. Then the impact of frequency changes on a particular tissue is compared to the past literature.

3. SAR variation in different homogeneous models due to a fixed input frequency and power

In this stage the previous stages which were carried out for all of the 6 tissue types, are used to estimate the relevant penetration depths and then listed in table 2. In this stage we can have some discussions on the responses of different tissues in accordance with their dielectric properties. That could be based on either of the fixed conditions in table 2.

4. SAR variation in multi layered models due to a special input power and frequency

During this stage, models of 5 and 6 layers are exposed respectively to the plane wave with the frequency 900 MHz, and the input power of 2 W. The 5 layered model includes skin (wet), fat (not infiltrated), bone (cortical), brain (grey matter) and brain (white matter), whereas the 6 layer model has an extra layer of 4 mm bone (cancellous), and the cortical layer thickness is decreased to 2 mm as illustrated in figure (1- b). Therefore the impact of the extra layer is inspected in this stage. The results are shown in figures (2-4). It should be mentioned that, the layers thicknesses are based on the ICRP standards [3]



(a)

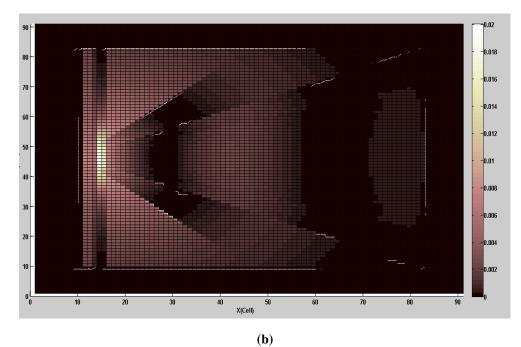
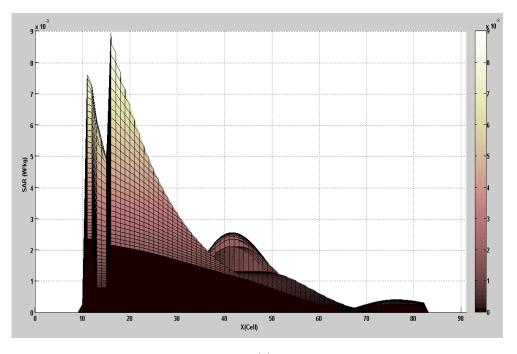
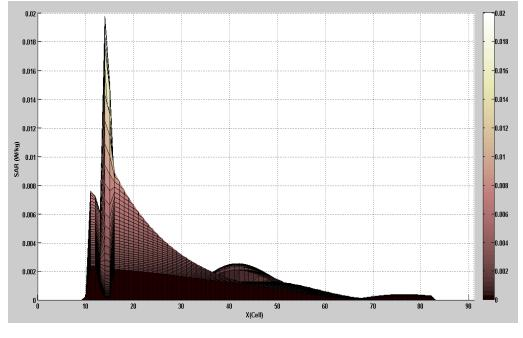


Figure2. Specific Absorption Rate (SAR) distribution in x- y plane passing through the source position for, (a) 5 layered model, (b) 6 layered model



(a)



(b)

Figure 3. Specific Absorption Rate (SAR) distribution in x-z plane passing through the source position for, (a) 5 layered model, (b) 6 layered model.

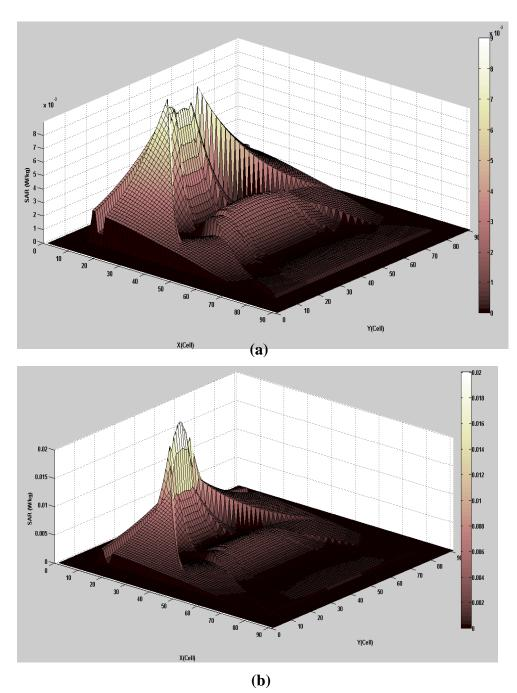


Figure 4. Specific Absorption Rate (SAR) 3 dimensional pattern in x- y plane passing through the source position for, (a) 5 layered model, (b) 6 layered model.

5. Penetration depth interpolation for a homogeneous model, based on SAR variations over the frequency range of 500- 2450 MHz

In this stage a simple homogeneous model of grey matter is exposed to a plane wave with the input power of 2 W, and over a wide radio frequency range. The frequency increments are determined to be 50 MHz, and the SAR distribution is plotted by MATLAB, in order to find penetration depth of the wave_ the distance at which the maximum energy absorption is decreased to the order of $1/e^2$ by the software's sampling tools [see figure 5]. The depths (cell numbers) are then plotted versus related frequencies. Finally, the whole trend is interpolated by the software's curve fitting tools [figures [6 (a, b)]]. The most appropriate curve fitting equation is as follow,

$$\delta = 66.08 f^{-0.9987} + 0.01978 \tag{13}$$

That could be considered as

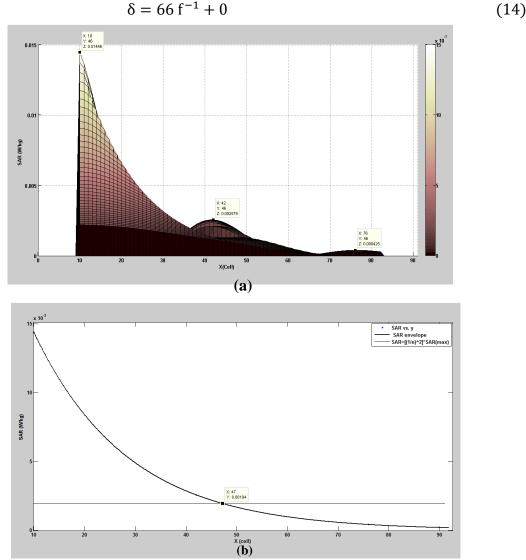


Figure 5. (a) Specific Absorption Rate (SAR) distribution in a simple model filled with grey matter at (900 MHz, 2 W) exposure. The data tips represent the samples used for predicting of envelop; (b) the relevant penetration depth is found at the crossing of the horizontal line and the curve (These procedures are carried out to estimate penetration depths in stages 1-3 and 5)

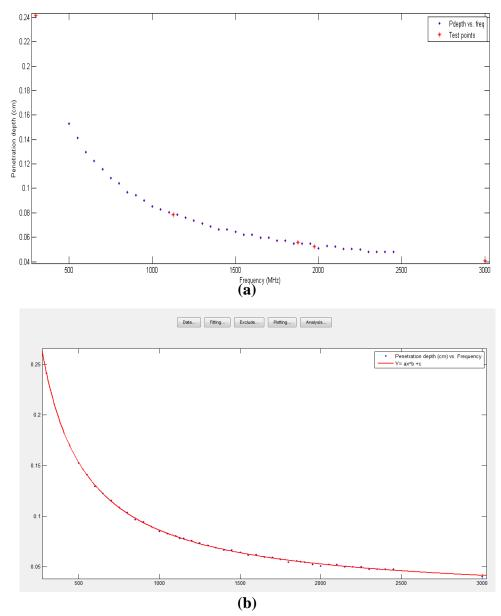


Figure6. Penetration depth (cm) trend in the frequency range 500- 2450 MHz. (a) The dots are the data gathered in stage 5 from grey matter as a lossy dielectric material, the solid line is achieved by curve fitting, (b) the asterisks are extra data to examine the accuracy of the fitted curve

Discussion and Conclusion

In the first stage, the increase in the input power shows an increase in the SAR inside the model. This includes all the cubical cells, and the most SAR is seen at the source position, while it decreases gradually in the adjacent cells. The penetration depth is fixed in both cases. In the second stage, the increase in the source frequency causes an increase in the SAR inside the model in a way that the penetration depth decreases. This is in complete agreement to the results obtained computationally by Keshvari et al on the realistic head models [17].

In stage 3, the analysis of the data shows that all the samples have similar response to the initial exposure conditions, and their dielectric parameters could lead to different energy distributions. According to [18, 15] biological tissues with low water content (low conductivity and permittivity), have reduced attenuation comparatively to those of high water content; consequently the wave have higher penetration depth inside the tissue. Here conductivity of cancellous is the greatest value among the other samples listed in table 1; while that of skin is the smallest value. Therefore, the penetration depth is also expected to be the least for cancellous, and the most for the skin (wet).

In stage 4, the presence of cancellous in 6 layered model causes high local energy deposition of 0.02 W/ kg in this layer, while the SAR distribution is the same in the other layers comparing to 5 layered model. This result could be compared with the others achieved computationally [19, 2, 15, 14], regarding the differences in input wave and tissue dielectric properties.

In the last stage, the penetration depth of a typically lossy dielectric material is interpolated by fitting different curves to the gathered data. Few extra data are entered later as test points to check the validity of the result. The trend shows a correlation to the input frequency, and this is in line with the expressions introduced for lossy dielectric materials in electromagnetic reference books.

Tissue type			
	ε [4]	σ (S/m)[4]	ρ (kg/m ^B)
Skin (dry) *	4	0.0002	1090 [15]
Skin (wet)	4	0.0004	1090 [15]
Fat (infiltrated) *	2.5	0.0350	950 [15]
Fat (not infiltrated)	2.5	0.0100	950 [15]
Bone (cancellous)	2.5	0.07	1180 [15]
Bone (cortical)	2.5	0.02	1920 [15]
Brain (grey matter)	4	0.02	1038.5 [2]
Brain (white matter)	4	0.02	1043.3 [2]

Table1. Dielectric	parameters used	in this study.(*	*: Extra information)
			·

Image: section of the secti	Tissue	Freq. (MHz)	Power (W)	SAR _{max}	SAR p. depth	Penetration depth (Cell	Penetration depth
LetLetLetLetLetWhite matter900214.01.94489.6Grey matter900215.01.95489.6Bone (Carcellous)900245.06.02224.4Bone (Carcical)90027.81.05408.0Fat (not matter90027.91.066913.8*Skin (wet)90020.30.04 $\gg73$ $\gg14.6**$ white matter90017.20.98489.6Grey matter90017.30.98489.6Bone (Carciellous)900122.03.02224.4Bone (Carciellous)90013.90.53408.0Bone (Carciellous)90010.10.02 $\gg73$ $\gg14.6**$ White matter1800215.01.95295.8Skin (wet) Matter90021.06413.2Skin (wet) 		(141112)	(**)	(W/kg) × 10 ⁻³	$(W/k_{C}) \times 10^{-3}$		I ⁸ (cm) ≅ cell No. ×
White matter 900 2 14.0 1.94 48 9.6 Grey matter 900 2 15.0 1.95 48 9.6 Bone (Cancellous) 900 2 45.0 6.02 22 4.4 Bone (Cortical) 900 2 7.8 1.05 40 8.0 Fat (not infiltrated) 900 2 7.9 1.06 699 13.8* Skin (wet) 900 2 0.3 0.04 >>73 >>14.6** white infiltrated) 900 1 7.3 0.98 48 9.6 Skin (wet) 900 1 7.3 0.98 48 9.6 Bone (Carcellous) 900 1 7.3 0.98 48 9.6 Bone (Carcellous) 900 1 7.3 0.98 48 9.6 Bone (Carcellous) 900 1 3.9 0.53 40 8.0 Skin (wet) 900 1 0.1 <th></th> <th></th> <th></th> <th><math>(\mathbf{w}/\mathbf{kg}) \times 10</math></th> <th>$(W/Kg) \times 10$</th> <th>,</th> <th>$[o(cm) \equiv cen wo.x]$</th>				$(\mathbf{w}/\mathbf{kg}) \times 10$	$(W/Kg) \times 10$,	$[o(cm) \equiv cen wo.x]$
White matter 900 2 14.0 1.94 48 9.6 Grey matter 900 2 15.0 1.95 48 9.6 Bone (Cancellous) 900 2 45.0 6.02 22 4.4 Bone (Cortical) 900 2 7.8 1.05 40 8.0 Fat (not infiltrated) 900 2 7.9 1.06 699 13.8* Skin (wet) 900 2 0.3 0.04 >>73 >>14.6** white infiltrated) 900 1 7.3 0.98 48 9.6 Skin (wet) 900 1 7.3 0.98 48 9.6 Bone (Carcellous) 900 1 7.3 0.98 48 9.6 Bone (Carcellous) 900 1 7.3 0.98 48 9.6 Bone (Carcellous) 900 1 3.9 0.53 40 8.0 Skin (wet) 900 1 0.1 <th></th> <th></th> <th></th> <th></th> <th></th> <th></th> <th></th>							
matter Grey matter 900 2 15.0 1.95 48 9.0 Bone (Cancellous) 900 2 45.0 6.02 22 4.4 Bone (Cortical) 900 2 7.8 1.05 40 8.0 Fat (not infiltrated) 900 2 7.8 1.05 69 13.8* Skin (wet) 900 2 0.3 0.04 >>73 >>14.6** White matter 900 1 7.2 0.98 48 9.6 Bone (Carcellous) 900 1 7.3 0.98 48 9.6 Bone (Carcellous) 900 1 7.3 0.98 48 9.6 Bone (Carcellous) 900 1 7.3 0.98 48 9.6 Bone (Carcellous) 900 1 3.9 0.53 40 8.0 Skin (wet) 900 1 0.1 0.02 >73 >>14.6** White matter 800 2							
Grey matter 900 2 15.0 1.95 48 9.6 Bone (Cancellous) 900 2 45.0 6.02 22 4.4 Bone (Cortical) 900 2 7.8 1.05 40 8.0 Fat (not infiltrated) 900 2 7.9 1.06 69 13.8* Skin (wet) 900 2 0.3 0.04 >>73 >>14.6** white matter 900 1 7.2 0.98 48 9.6 Bone (Cortical) 900 1 7.3 0.98 48 9.6 Bone (Cortical) 900 1 7.3 0.98 48 9.6 Bone (Cortical) 900 1 22.0 3.02 22 4.4 Skin (wet) 900 1 3.9 0.53 40 8.0 Grey (Cortical) 900 1 0.1 0.02 >73 >14.6** White infiltrated) 1800 2 15		900	2	14.0	1.94	48	9.6
matter imatter imatter <t< th=""><th></th><th></th><th></th><th>1 7 0</th><th>1.05</th><th>10</th><th>0.4</th></t<>				1 7 0	1.05	10	0.4
(Cancellous) \sim <		900	2	15.0	1.95	48	9.6
Bone (Cortical) 900 2 7.8 1.05 40 8.0 Fat (not infiltrated) 900 2 7.9 1.06 69 13.8* Skin (vet) 900 2 0.3 0.04 >>73 >>14.6** white matter 900 1 7.2 0.98 48 9.6 Grey matter 900 1 7.3 0.98 48 9.6 Bone (Cancellous) 900 1 22.0 3.02 22 4.4 Bone (Cortical) 900 1 3.9 0.53 400 8.0 Fat (not infiltrated) 900 1 4.0 0.54 69 13.8* Skin (vet) 900 1 0.1 0.02 >>73 >>14.6** white infiltrated) 1800 2 14.0 1.94 29 5.8 Bane (Cancellous) 1800 2 15.0 1.95 29 5.8 Bane (Cancellous) 1800 2 <th>Bone</th> <th>900</th> <th>2</th> <th>45.0</th> <th>6.02</th> <th>22</th> <th>4.4</th>	Bone	900	2	45.0	6.02	22	4.4
$\begin{array}{ c c c c c c } \hline Cortical & & & & & & & & & & & & & & & & & & &$							
Fat (not infiltrated) 900 2 7.9 1.06 69 13.8* Skin (vet) 900 2 0.3 0.04 >>73 >>14.6** white matter 900 1 7.2 0.98 48 9.6 Grey matter 900 1 7.3 0.98 48 9.6 Bone (Carcellous) 900 1 22.0 3.02 22 4.4 Bone (Carcellous) 900 1 22.0 3.02 22 4.4 Bone (Carcellous) 900 1 22.0 3.02 22 4.4 Bone (Carcellous) 900 1 4.0 0.53 40 8.0 Skin (wet) 900 1 0.1 0.02 >73 >14.6** white matter 1800 2 14.0 1.94 29 5.8 Matter 1800 2 15.0 1.95 29 5.8 Bone (Carcellous) 1800 2 7.8 </th <th></th> <th>900</th> <th>2</th> <th>7.8</th> <th>1.05</th> <th>40</th> <th>8.0</th>		900	2	7.8	1.05	40	8.0
Skin (wet) 900 2 0.3 0.04 >>73 >>14.6** white matter 900 1 7.2 0.98 48 9.6 Grey matter 900 1 7.3 0.98 48 9.6 Bone (Cancellous) 900 1 22.0 3.02 22 4.4 Bone (Cancellous) 900 1 22.0 3.02 22 4.4 Bone (Cancellous) 900 1 3.9 0.53 40 8.0 Fat (not infiltrated) 900 1 4.0 0.54 69 13.8* Skin (wet) 900 1 0.1 0.02 >>73 >>14.6** white matter 1800 2 14.0 1.94 29 5.8 Grey matter 1800 2 15.0 1.95 29 5.8 Bone (Cancellous) 1800 2 7.8 1.05 25 5.0 Grey matter 1800 2 7.9<		900	2	7.9	1.06	69	13.8*
white matter 900 1 7.2 0.98 48 9.6 Grey matter 900 1 7.3 0.98 48 9.6 Bone (Cancellous) 900 1 22.0 3.02 22 4.4 Bone (Cancellous) 900 1 22.0 3.02 22 4.4 Bone (Cancellous) 900 1 3.9 0.53 40 8.0 Fat (not infiltrated) 900 1 4.0 0.54 69 13.8* Skin (wet) 900 1 0.1 0.02 >>73 >>14.6** white matter 1800 2 15.0 1.95 29 5.8 Matter 1800 2 7.8 1.05 25 5.0 Bone (Cancellous) 1800 2 7.9 1.06 41 8.2*							
matter Imatter Imatter <thimatter< th=""> Imatter <thimatter< th=""> <thimatter< th=""> <thima< th=""><th>Skin (wet)</th><th>900</th><th>2</th><th></th><th>0.04</th><th></th><th>>>14.6**</th></thima<></thimatter<></thimatter<></thimatter<>	Skin (wet)	900	2		0.04		>>14.6**
Grey matter 900 1 7.3 0.98 48 9.6 Bone 900 1 22.0 3.02 22 4.4 (Cancellous) 900 1 22.0 3.02 22 4.4 Bone 900 1 3.9 0.53 40 8.0 (Cortical) 900 1 4.0 0.54 69 13.8* skin (wet) 900 1 0.1 0.02 >>73 >>14.6** white 1800 2 14.0 1.94 29 5.8 matter 900 1 0.1 0.02 >>73 >>14.6** Matter 900 2 15.0 1.95 29 5.8 Bone 1800 2 7.8 1.05 25 5.0 Bone 1800 2 7.8 1.05 25 5.0 Fat (not infiltrated) 1800 2 7.9 1.06 41 8.2*		900	1	7.2	0.98	48	9.6
matter Imatter Imatter <thimatter< th=""> <thimatter< th=""> <thim< th=""><th></th><th>900</th><th>1</th><th>7.3</th><th>0.98</th><th>48</th><th>9.6</th></thim<></thimatter<></thimatter<>		900	1	7.3	0.98	48	9.6
(Cancellous) Image: Constraint of the second s							
Bone 900 1 3.9 0.53 40 8.0 (Cortical) 900 1 4.0 0.54 69 13.8* Fat (not infiltrated) 900 1 0.1 0.02 >>73 >>14.6** Skin (wet) 900 1 0.1 0.02 >>73 >>14.6** white 1800 2 14.0 1.94 29 5.8 matter	Bone	900	1	22.0	3.02	22	4.4
(Cortical) Image: Cortical of the sector of th	(Cancellous)						
Fat (not infiltrated) 900 1 4.0 0.54 69 13.8* skin (wet) 900 1 0.1 0.02 >>73 >>14.6** white 1800 2 14.0 1.94 29 5.8 matter - - - - - - Grey 1800 2 15.0 1.95 29 5.8 Matter - - - - - - Bone 1800 2 45.0 6.02 16 3.2 Bone 1800 2 7.8 1.05 25 5.0 fat (not 1800 2 7.9 1.06 41 8.2*		900	1	3.9	0.53	40	8.0
infiltrated) Image: Skin (wet) 900 1 0.1 0.02 >>73 >>14.6** Skin (wet) 900 1 0.1 0.02 >>73 >>14.6** white 1800 2 14.0 1.94 29 5.8 matter Image: State of the s	· · /			1.0	0.54	10	10.01
Skin (wet) 900 1 0.1 0.02 >>73 >>14.6** white 1800 2 14.0 1.94 29 5.8 matter - - - - - - - Grey 1800 2 15.0 1.95 29 5.8 Matter - <th< th=""><th></th><th>900</th><th>1</th><th>4.0</th><th>0.54</th><th>69</th><th>13.8*</th></th<>		900	1	4.0	0.54	69	13.8*
white matter 1800 2 14.0 1.94 29 5.8 Grey 1800 2 15.0 1.95 29 5.8 Matter 1800 2 45.0 6.02 16 3.2 Bone 1800 2 7.8 1.05 25 5.0 Grey Matter 1800 2 7.8 1.05 25 5.0 Bone 1800 2 7.9 1.06 41 8.2*		900	1	0.1	0.02	>>73	>>14.6**
matter Image: Constraint of the symbol of the		1800	2	14.0			
Matter Image: Constraint of the state of th	matter						
Bone (Cancellous) 1800 2 45.0 6.02 16 3.2 Bone 1800 2 7.8 1.05 25 5.0 (Cortical) 7 1.06 41 8.2* infiltrated) 8 1.06 41 8.2*	Grey	1800	2	15.0	1.95	29	5.8
(Cancellous) Image: Cancellous of the second s							
Bone (Cortical) 1800 2 7.8 1.05 25 5.0 Fat (not infiltrated) 1800 2 7.9 1.06 41 8.2*		1800	2	45.0	6.02	16	3.2
(Cortical) Image: Cortical of the second secon	· · /	1000		- 0	1.07		
Fat (not infiltrated) 1800 2 7.9 1.06 41 8.2*		1800	2	7.8	1.05	25	5.0
infiltrated)		1000	2	7.0	1.00	41	0.7*
		1800	2	1.9	1.06	41	ð.∠*
Skin (wet) 1800 2 0.3 0.04 $>>73 >>14.6**$	Skin (wet)	1800	2	0.3	0.04	>>73	>>14.6**

 Table2. Specific Absorption Rate (SAR) variation in simple cubic models of tissues due to

 different initial conditions

Penetration depth is estimated for each sample for further discussions.

*: The penetration depth is quite large in comparison to the model size.

**: The penetration depth is not achievable inside the model.

To put in a nutshell, the aim of this study was to model and simulate the interaction of electromagnetic waves with the human tissues, and comparing the results with the achievements of others, obtained by investigating anatomically detailed models. The results obtained show us, considering human head tissues as dispersive materials obeying equation (9), it is possible to say that the multi planar layered model is useful to estimate energy deposition in cases that precise calculations are not of major importance. Moreover, according to the correct results, complicated specifications could be imposed in case of further research.

References

- 1. Y. Liu, "Review on the Investigation of the Mechanism of the Biological Effects of the Electromagnetic Radiation", Basic Medical Sciences and Clinics, 1 (2000).
- M. C. Gosseline, S. Kuhn, P. Crespo Valero, E. Cherubini., M. Zefferer, A. Christ, N. Kuster, "Estimation of head tissue-specific exposure from mobile phones basedon measurements in the homogeneous SAM head", Bioelectromagnetics, 10 (2011) 1002/bem.20662.
- 3. ICRP 1994 Human Respiratory Tract Model for Radiological Protection ICRP Publication 66.
- P. J. Dimbylow, "FDTD Calculations of the Whole-Body Averaged SAR In an Anatomically Realistic Voxel Model of the Human Body from 1 MHz to 1 GHz", Phys. Med. Biol., 42 (1996) 479-90.
- P. Dimbylow, "Development of the Female Voxel Phantom, NAOMI, and Its Application to Calculations of Induced Current Densities and Electric Fields from Applied Low Frequency Magnetic and Electric Fields", Phys. Med. Biol., 50 (2005) 1047-1070.
- 6. T. Nagaoka, S. Watanabe, K. Sakurai, E. Kuneida, S. Watanabe, M. Taki, Y. Yamanaka, "Development of Realistic High-Resolution Whole-Body Voxel Models of Japanese Adult Males and Females of Average Height and Weight, and Application of Models to Radio-Frequency Electromagnetic-Field Dosimetry", Phys. Med. Biol., 49 (2003) 1-15.
- S. Gabriel, R. W. Lau, C. Gabriel, "The Dielectric Properties of Biological Tissues: III. Parametric Models for the Dielectric Spectrum of Tissues", Phys Med Biol., 41 (1996) 2271-2293.
- S. Gabriel, R. W. Lau, C. Gabriel, "The Dielectric Properties of Biological Tissues: II. Measurements in the Frequency Range 10 Hz to 20 GHz", Phys Med Biol., 41(1996) 2251-2269.
- 9. K. S. Yee, "Numerical solution of initial boundary value problems involving Maxwell's equations in isotropic Media", IEEE Trans. Antennas Propag, 14 (1966) 302-7.

- J. P. Berenger, "Three Dimensional Perfectly Matched Layer for the Absorption of Electromagnetic Waves", J. Comput. Phys., 127 (1996) 363-379.
- J. W. Hand, "Modeling the Interaction of Electromagnetic Fields (10 MHz- 10 GHz) with the Human Body: Methods and Applications (Topical Review)", Phys. Med. Biol., 53 (2008) 243-286.
- L. J. Challis, "Mechanism for Interaction between RF Fields and Biological Tissues (Review)", Bioelectromagnetics Supplement, 7 (2005) 98-106.
- F. S. Barnes, B. Greenebaumw, "Handbook of Biological Effects of Electromagnetic Fields, BBA", Third Edition, CRC Press (2006).
- M. A. Kelsh, M. Shum, A. R. Sheppard, M. McNeely, N. Kuster, E. Lau, R. Weidling, T. Frdyce, S. Kuhn, TH. Sulser, "Measured radiofrequency exposure during various mobile-phone use scenarios.", J Expo Sci Environ Epidemiol., 10 (2010), 1038/jes.2010.12.
- A. Christ, M. Ch. Gosseline, M. Christopoulou, S. Kuhn, N. Kuster, "Age Dependent Tissue specific Exposure of Cell Phone Users", Phys Med Biol., 7 (2010) 1767-1783.
- H. Virtanen, J. Keshvari, R. Lappalainen, "The Effect of Authentic Metallic Implants on the SAR Distribution of the Head Exposed to 900, 1800 and 2450 MHz Near Field", Phys. Med. Biol., 52 (2006) 1221-1236.
- 17. J. Keshvari, S. Lang, "Comparison of Radio Frequency Absorption in Ear and Eye Region of Children and Adults at 900, 1800 and 2450 MHz", Phys. Med. Biol., 50 (2005)4355-4369.
- A. Christ, T. Samaras, A. Klingenbock, N. Kuster, "Characterization of the Electromagnetic Near- Field Absorption in Layered Biological Tissue in the Frequency Range from 30 MHz to 6000 MHz", Phys. Med. Biol., 51 (2006) 4951-4965.
- V. Anderson, "Comparisons of Peak SAR Levels in Concentric Sphere Head Models of Children and Adults for Irradiation by a Dipole at 900 MHz", Phys. Med. Biol., 48 (2003) 3263-3275.